

https://dspace.org/

Heavy mesons in the bag model

Davidson, Neil John

2015-01-19
http://hdl.handle.net/10539/16602

Downloaded from a DSpace repository. https://dspace.org/

HEAVY MESONS IN THE BAG MODEL

Neil John Davidson

A dissertation submitted to the Faculty of Science, University of the Witwatersrand, in fulfilment of the requirements for the degree Master of Science.

Johannesburg, 1988.

ABSTRACT

The MIT bag model has been widely applied to light quark systems, but has rarely been used to study heavy quark systems. For the bag model to be consistent for describing particles composed of quarks, it should be able to predict the spectra of heavy quark systems as well. In this dissertation, a non-relativistic bag model is developed, incorporating a soft bag approach to confinement through a phenomenological non-square well potential. The gluons are confined to the same soft bag as the quarks. This model is then used to calculated the $J^P=1^-$ spectra of the J/ψ and Υ mesons.

The non-relativistic nature of heavy quark systems permits the use of Schroedinger and Maxwell equations for the generation of the single quark and gluon modes respectively. In addition, only the static part of the interaction need to be included in the Hamiltonian.

The meson spectra are calculated using effectively three free parameters, and are compared to both experimental observations and the results of potential model calculations. The non-relativistic soft bag model is shown to provide results that are of an accuracy comparable to that of the potential models, and are in good agreement with experiment.

DECLARATION

I declare that this dissertation is my own, unaided work. It is being submitted for the degree of Master of Science in the University of the Witwatersrand, Johannesburg. It has not been submitted before for any other degree or examination in any other University.

.....

15th day of September, 1988

ACKNOWLEDGEMENTS

Many thanks to Dieter Heiss, my supervisor, for his guidance and encouragement, and the many hours of discussion over the past years.

I thank David Eyre for discussions on the form of the soft confinement.

Also, I thank Hank Miller, Rachel Carter and Johnathan Quick for useful discussions and the loan of computer routines.

I also thank Maureen Taverner for typing this dissertation, and Ann Strauss and Torill Karlsen for proofreading.

CONTENTS

		Page No.
1.	INTRODUCTION	1
2.	THE MODEL FOR q-$\bar{q}$ SYSTEMS	4
	2.1 The bag model for single gluon exchange in relativistic systems	4
	2.2 The non-relativistic approximation for the q/$\bar{q}$ modes	10
	2.3 The gluon modes	12
	2.4 The effect of the non-relativistic approximation on the Hamiltonian	13
	2.5 The soft bag	14
	2.6 The quark, antiquark and gluon modes in a soft bag	19
	2.7 The vertex integrals $s^{(n)}$ for the soft bag model	24
	2.8 The coupling of the angular momenta	26

		Page No.
3.	THE STATES FOR J/ψ AND T MESONS	27
3.1	The parameters for the model	27
3.2	The method of fitting the data	28
3.3	The choice of the confining potential	30
3.4	The single quark/antiquark states	33
3.5	The gluon states	37
3.6	The calculation of the interaction term $U_{14,32}$	39
3.7	The J/ψ spectrum	39
3.8	The T spectrum	43
3.9	The RMS radii of the mesons and the quark masses	46
3.10	Comparison of the soft bag model with potential models	50
3.11	The meson wave functions in the soft bag model	56
4.	CONCLUSIONS	58
APPENDIX A:	The meson wavefunctions	62
REFERENCES		66

LIST OF TABLES

3.1	Step positions and values of κ	31
3.2	Step positions and values for the confining potential V	32
3.3	Single quark/antiquark energies for the J/ψ meson for the potential of Table 3.2	34
3.4	Single quark/antiquark energies for the T meson for the potential of Table 3.2	35
3.5	Single quark/antiquark energies for the J/ψ meson for a hard bag	35
3.6	Single quark/antiquark energies for the ψ meson for a hard bag	36
3.7	Gluon modes for κ as in Table 3.1	37
3.8	Gluon modes in a hard bag	38
3.9	J/ψ states for various β, for the potential of Table 3.2 and for a hard bag	40
3.10	Experimental J/ψ states	41
3.11	T states for various β, for the potential of Table 3.2	44
3.12	Experimental T states	45
3.13	RMS radii for the J/T spectrum	48
3.14	RMS radii for the T spectrum	49

LIST OF FIGURES

2.1	Diagrams for contributions of Eqs. (6), (7) and (8)	10
2.2	Diagrammatic form of the Hamiltonians (13) and (14) respectively	15
2.3	Radial dependence of κ for a hard bag	16
2.4	Proposed radial dependence of κ for a soft bag	16
2.5	Stepped construction of κ (r)	17
3.1	The chosen confining potential V(r)	33
3.2	Experimental, soft bag and power law potential model results for the J/ψ meson spectrum	52
3.3	Experimental, soft bag and coulomb and power law potential model results for the J/ψ meson spectrum	53
3.4	Experimental, soft bag and power law potential model results for the T meson spectrum	54
3.5	Experimental, soft bag and coulomb and power law potential model results for the T meson spectrum	55

NOTATION

κ	Dielectric constant
κ_i	Steps in dielectric constant
ω_n^T	Transverse gluon eigenvalue
ω_n^L	Longitudinal gluon eigenvalue
G_{ij}	Gluon propagator
$\Delta_{14,32}$	Energy dependedent part of interaction
ϵ_i	Single particle quark energy
δ_i	Single particle antiquark energy
$\Sigma_{14,32}$	Self energy part of interaction
$U_{14,32}$	Static part of interaction
δ_{ij}	Kronecke delta
ψ	Single quark/antiquark wave function
$\vec{E}$	Colour electric field
$\vec{B}$	Colour magnetic field
$H_{14,32}$	Hamiltonian
g_s	Strong coupling constant
α_s	Coupling constant
c_s	Speed of light in vacuum
$V(r)$	Confining potential
V_i	Steps in confining potential
m	Quark mass

β	Mass scaling factor
R	Bag radius
R_f	Step position within bag
V_0	Potential softening strength
$R_\ell(r)$	Radial quark/antiquark wave function
$\phi_\ell(r)$	Radial gluon wavefunction
$Y_\ell^m(\Omega)$	Spherical harmonic
$\hbar$	Planck's constant divided by 2π
c	Charm
b	Bottom
ℓ	Orbital angular momentum
s	Spin angular momentum
J	Total angular momentum
P	Parity
E_j	Meson energy
c_{ij}	Single particle component of collective state eigenvector

1. INTRODUCTION

The postulate of the quark model for hadrons in the late 1960s has led to various attempts being made to determine the theoretical background to hadron structure in terms of quarks and gluons. The most favourable theory for providing a description of the strong interaction is that of quantum chromodynamics (QCD). Lee[1] provides an introduction to this theory. However, QCD is a complex theory, and phenomenological models have been developed to explain the quark structure of matter.

The two most important groups of these phenomenological attempts are the bag models (MIT[2] and SLAC[3]), and the potential models (for reviews see [18], [28]). The two groups differ in that while the bag models are based on quantum chromodynamics, the potential models have their grounding in relativistic or non-relativistic quantum mechanics. The bag models consider the quarks to be confined to a region of space, and to interact via an exchange of gluons. The potential models, on the other hand, view both the confinement of the quarks and their interaction as a single potential in the Dirac or Schroedinger equation.

The potential models, however, do not prove to be entirely satisfactory as a means of describing baryons or light mesons[4]. They have been widely used, however, in the study of heavy quark systems, and have proved to provide reliable and accurate results for systems such as the J/ψ and T mesons [20], [22], [23]. This is the opposite of the situation that has occurred with the bag models, which give good results for the light quark systems, but have rarely been applied to heavy quark systems. It is

desirable that for the *bag* to be acceptable as a general model, it should be consistent, and produce good results for heavy quark systems. It is the intention of this dissertation to show that the bag model can provide acceptable results for the heavy J/ψ and Υ systems.

The use of heavy quarks allows certain approximations to be made to the bag model used in the analysis of light quark systems [2], [5], [6]. The basis of these approximations is the non-relativistic nature of the problem, which allows simplification of both the single particle modes and the gluon-mediated interaction.

In this non-relativistic approach to heavy mesons we ultimately use a particle-hole model as in traditional nuclear physics. We assume a reservoir of quarks, with the vacancies in this reservoir being the antiquarks. Throughout this dissertation, we shall consider the mesons to consist of single quark - single antiquark states; a more complete treatment would have to take multiple quark - multiple antiquark states into account.

In Chapter 2, we give a brief review of a single gluon mediated relativistic bag theory using the formulism of [5] and [6], and then introduce the approximations mentioned above to this model to obtain a non-relativistic model for a quark-antiquark pair in a bag. The approximations also require us to introduce a scaling factor on the mass to obtain the correct radial dependence of the meson states.

We also introduce the concept of a soft bag in this chapter. The bag model as originally formulated[1] makes use of an "infinite square well" form of bag. Various authors (see for example [7]) have made use of other

confining potentials, in particular potentials of the form $V(r) \sim r^2$ or $V(r) \sim r^3$. We propose a more flexible method of softening the bag, which, while retaining the computational simplicity of the square well, allows us to mimic the r^2 or r^3 bag used in the literature. The proposed method has a similar effect on state ordering as the r^n bag when compared to the square well bag, i.e. higher ℓ states are shifted up more than lower ℓ states. In addition, we show that gluons can be treated in the same bag as the quarks, which is physically appealing, albeit phenomenological.

The non-relativistic soft bag model is applied to the J/ψ and Υ systems in Chapter 3. A phenomenological confining potential is proposed, and the spectra for the J/ψ and Υ mesons calculated using this potential. The model is dependent on only three parameters, namely the bag radius, the coupling constant and the mass scaling factor for each meson, apart from the choice of parameters for the potential. In addition to the spectra, we find the RMS radii of the mesons, as well as masses for the charm and bottom quarks from the best fit for the spectra. The model results are compared to both experimental observations and the predictions of potential models. In Chapter 4, we draw conclusions from the results, and suggest improvements to the model.

2. THE MODEL FOR q-$\bar{q}$ SYSTEMS

It is useful to start the description of the model used in this dissertation by examining the bag model for relativistic systems with single gluon exchange, before adapting the equations and formulism to deal with non-relativistic systems.

2.1 The bag model for single gluon exchange in relativistic systems

The bag model was originally postulated by Chodos et al.[2] as a phenomenological approach to the question of the non-observability of free quarks. It introduces the concept of confinement of the quarks. This is achieved by assuming that a strongly interacting particle is confined to a finite region of space with a constant energy density, within which the included fields (fermions or bosons) are constrained. The assumption of constant energy density ensures that the confinement is Lorentz-invariant.

An analogy for the bag model can be found in classical electromagnetism[1]. Consider the case of a normal dielectric medium with dielectric constant $\kappa>1$, as is required for all physical media.

We now attempt to isolate a charge e^+ within the dielectric, and to create a "bag" of vacuum around the charge. As a result of the positive charge in the cavity, a negative charge is induced on the inner surface of the cavity. This is known as the screening characteristic of dielectrics.

Owing to simple Coulomb forces, the "bag" will collapse onto the positive charge. Thus it is clear that a dielectric medium cannot support a vacuum within the structure.

We now assume the existence of a dia-electric *medium*; that is, an anti-screening material. This requires a dielectric constant $\kappa<1$, to ensure that the induced charge is of the same sign as the charge in the centre of the cavity. The repulsion of the two like-signed charge distributions ensures that the bag does not collapse, but maintains a finite size.

Quark confinement can be viewed in similar terms to the above anti-screening situation. We begin by replacing the idea of electric charge by that of colour charge e_c. We then view the QCD vacuum as a perfect colour dia-electric medium. We then obtain the result that whenever quarks or antiquarks are present, an inhomogeneity must appear in the space surrounding the particles. It is this inhomogeneity that is called the bag. Within the bag, $\kappa=1$, while outside, $\kappa=0$, or at least is very much less than 1.

Lee shows[1] that the total energy of the classical electromagnetic system is given by

$$M \sim {}^{4}/_{3} \quad \left(\frac{e^2}{2\kappa_{med}}\right)^{3/4} \quad (4\pi p)^{1/4} \qquad (1)$$

where p is a positive constant. It is clear from the above description that for $e\neq0$, the radius of the bag $R\neq0$. Also, it is obvious that the energy of such a system becomes infinite as κ_{med} tends to 0.

We now replace the single electromagnetic charge distribution by a dipole of equal but opposite charges, spatially separated. Again the minimum energy state for $\kappa_{med}<<1$ requires the existence of a "hole" in the medium[1]. Thus, despite the fact that the total charge is zero in this case, the bag remains finite due to the separation of the charge distributions.

The same argument can be applied to colour charges. To obtain finite masses for the hadrons, it is necessary to have a colour singlet within the bag composed of separate colour charge distributions. In this case, $e_c=0$ and the mass of the bag may remain finite for $\kappa_{med}\neq 0$ by the same argument as that for the EM case above. We are thus in a position to describe the mesons by $q^i\bar{q}^i$ states where i is a colour index.

It can also be shown[1] that the flux lines within the bag for a colour dipole of the form encountered in mesons must be parallel to the surface of the bag at the surface so that the flux outside the bag is indentically 0 as is appropriate for a dia-electric medium. Also, infinite energy is required for the separation of the dipole. This explains the confinement of quarks and antiquarks within the bag.

The quark/antiquark interaction is mediated by gluon exchange. The actual form of the interaction is not prescribed by the bag model[5]. The interaction must, however, bring about collectivity within the bag. For the purposes of this dissertation, only single gluon mediation of the interaction will be considered. It is also assumed that the gluons are restricted to the same bag as the quark/antiquark pair. Gluon self-interaction is not considered, as the assumption of a bag supposedly includes this interaction[5].

The assumption of a confining potential introduces spurious centre of mass motion. However, the effect of this motion is small in the case of light quark systems [6], and negligible in heavy quark systems. In this dissertation, centre of mass motion is thus not considered.

In the bag model the quark and antiquark energies and wavefunctions may be found from the positive and negative energy solutions respectively, of the Dirac equation for a bag of radius R

$$(i\gamma\partial - m)\,\psi = 0, \quad r < R \tag{2}$$

with the boundary condition[8]

$$-i\vec{\gamma}\cdot\hat{r}\psi = \psi \text{ at } r = R.$$

We treat the gluons like photons in QED. The gluon self-interaction inherent in QCD is left out as discussed above. We choose to work in the Coulomb gauge to obtain a static interaction in the non-relativistic limit in a natural way. We thus obtain the gluon modes from the solution of Maxwell's equations in a cavity for a Coulomb gauge:

$$\begin{aligned} &[\nabla^2 + (\omega_n^T)^2]\ \vec{A}^{(n)} = 0 \\ &\nabla \cdot \vec{A}^{(n)} = 0 \end{aligned} \tag{3}$$

with the boundary conditions

$$\hat{r}\cdot\vec{E} = 0$$
$$\hat{r}\times\vec{B} = 0 \qquad \text{at } r=R,$$

where $\dot{A}$ gives rise to the dynamic portion of the gluon propagator

and

$$[\nabla^2 + (\omega_n^L)^2]\ \phi^{(n)} = 0 \tag{4}$$

for the static part ϕ^n, with boundary condition

$$\hat{r}\cdot\nabla\phi = 0 \qquad \text{at} \qquad r = R,$$

i.e. zero flux across the boundary.

The gluon propagator is given by[5]

$$\begin{aligned} G_{ik}(\omega) &= \sum_n \frac{A_i^{*(n)}(\vec{r})\, A_k^{(n)}(\vec{r}')}{\omega^2 - (\omega_n^T)^2} \\ G_{00}(\omega) &= -\sum_{n\neq 0} \frac{\phi^{*(n)}(\vec{r})\,\phi^{(n)}(\vec{r}')}{(\omega_n^L)^2} \end{aligned} \tag{5}$$

For one gluon exchange there are three terms to the interaction. The energy dependent part is of the form

$$\Delta_{14,32} = \sum_n \frac{[r_{13}^{(n)} r_{42}^{(n)}]_0}{\omega - \epsilon_3 + \delta_4 - \omega_n^T} + \sum_n \frac{[r_{42}^{(n)} r_{13}^{(n)}]_0}{\omega - \epsilon_1 + \delta_2 - \omega_n^T} \tag{6}$$

where ϵ and δ are quark and anti-quark energies respectively, $[]_J$ indicates coupling of the angular momenta of the channel considered to a total J, and

$$r_{13}^{(n)} = \frac{1}{\sqrt{2\omega_n'}} \int d^3x \ \psi_1^*(\vec{x}) \ \vec{\gamma} \ \psi_3(\vec{x}) \cdot \vec{A}^{(n)}(\vec{x}).$$

The self energy terms are given by

$$\Sigma_{14,32}(\omega) = \sum_{n,J} \frac{[r_{1J}^{(n)} r_{J3}^{(n)}]_J}{\omega-\epsilon_J+\delta_4-\omega_n'} \delta_{13}\delta_{24} + \sum_{n,J} \frac{[r_{4J}^{(n)} r_{J2}^{(n)}]_J}{\omega-\epsilon_1+\delta_J-\omega_n'} \delta_{13}\delta_{24} \quad (7)$$

The static part of the interaction is

$$U_{14,32} = \sum_{n\neq 0} \frac{[s_{13}^{(n)} s_{24}^{(n)}]_J}{(\omega_n')^2} \quad (8)$$

where $s_{13}^{(n)} = \int d^3x \ \psi_1^*(\vec{x}) \ \gamma_0 \ \psi_3(\vec{x}) \ \phi^{(n)}(\vec{x})$.

The corresponding diagrams for the above terms are shown in Fig. 2.1.

The meson states can now be found by diagonalization of the matrix

$$H_{14,32} = (\epsilon_1-\delta_4)\,\delta_{13}\delta_{24} - \frac{16}{3}\alpha_s \,(\Lambda_{14,32}(\omega)+\Sigma_{14,32}(\omega)+U_{14,32}) \quad (9)$$

where $\alpha_s = g_s^2/4\pi$ and the factor $16/3$ is due to the coupling to a colour singlet state[6].

The above procedure has been carried out for light mesons [5],[6] and found to yield satisfactory results. For heavy mesons, such as the J/ψ and T, certain simplifications can be made to the above.

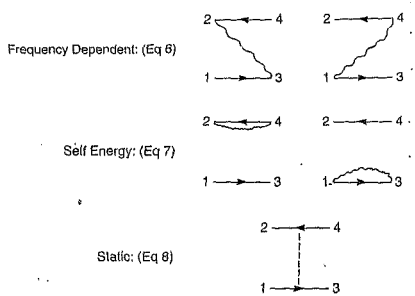

Fig. 2.1: Diagrams for contributions of Eqs. (6), (7) and (8)

2.2 The non-relativistic approximation for the $q/\bar{q}$ modes

In the case of the heavy quarks (charm, bottom and top), it is possible to view the system as being non-relativistic since the kinetic energy of the quarks is appreciably smaller than their mass, i.e.

$$p^2c_s^2 \ll m_0c_s^2$$

where p is the momentum of the quark and m_0 its rest mass. This means that instead of solving Dirac equations(2) for the $q/\bar{q}$ modes, we may solve the time-independent Schroedinger equation

$$\left[-\frac{\hbar^2\nabla^2}{2m} + V(\vec{r}) \right] \psi_n(\vec{r}) = \epsilon_n \psi_n(\vec{r}) \tag{10}$$

with the boundary conditions $\psi_n(R) = 0$
and $\psi_n(0)$ finite.

This solution is equivalent to the non-relativistic limit of the Dirac equation introduced in the previous section. Note that two boundary conditions are now necessary since the Schroedinger equation is second order, while the Dirac is first order.

In the non-relativistic equation (10), m is an effective mass. It is convenient to parameterize this mass by

$$m = \beta/R, \tag{11}$$

where R is the bag radius and β a constant. In our attempts to obtain a best fit to the meson spectra, we vary the parameter β rather than the mass m. The motivation for this parameterization is as follows: consider, for simplicity, an infinite, spherical well in (10). The radial solutions are then spherical Bessel functions $j_\ell(kr)$, where

$$k^2 = \frac{2m}{\hbar^2}\,\epsilon. \tag{12}$$

Since the energies of the solution are determined by the zeros of the j_ℓ, it is clear that $k = 1/R$, and thus that $\epsilon = 1/R^2$ if (11) is not used. However, it is well known that for solutions of the Dirac

equation, $\epsilon = 1/R$. The parameterization (11) thus ensures that the kinetic energy ϵ scales like the mass itself, i.e. inversely proportional to the bag radius, maintaining consistency with the relativistic case. The procedure for choosing β will be described later.

2.3 The gluon modes

By making the non-relativistic approximation, we are also able to simplify the procedure for generating the gluon modes. In the non-relativistic limit, only the integrals $s^{(n)}$ introduced in Section 2.1 survive, while the $r^{(n)}$ vanish, since the non-diagonal matrices γ mix the upper and lower components of the Dirac spinors. As a consequence, for light (relativistic) quarks, the vertex integrals $r^{(n)}$ and $s^{(n)}$ are of similar order, while for the case in question, i.e. that of heavy quarks, the $r^{(n)}$ integrals are smaller than the $s^{(n)}$ by a factor (E-m)/(E+m). In the case of the J/ψ and T mesons, this ratio is of the order of 0.3. This can be seen from the results given below where we find $m \sim 0.5\epsilon$. Since both the energy-dependent and self-energy terms are dependent on the product of two $r^{(n)}$ integrals, both terms are to good approximation less than 10% of the static term. Their exclusion from the Hamiltonian is thus justified.

The result of the setting $\vec{A} = 0$ is the disappearance from the model of transverse gluons. The longitudinal gluon modes are generated by (4), with only the G_{00} propagator being relevant.

2.4 The effect of the non-relativistic approximation on the Hamiltonian

The major effect on the Hamiltonian is brought about by the exclusion of the dynamic interaction from the model. As discussed above, both the energy dependent and self-energy terms disappear from the Hamiltonian (9) owing to the dynamic interaction $\bar{A}$ being zero.

The non-relativisitic Hamiltonian, after the exclusion of the energy-dependent and self-energy terms, is thus the sum of an unperturbed Hamiltonian

$$H^{un}_{14,32} = (\epsilon_1 - \delta_4)\, \delta_{13}\, \delta_{24} \tag{13}$$

and static interaction Hamiltonian

$$H^{int}_{14,32} = \frac{16}{3}\, \alpha_s\, U_{14,32} \tag{14}$$

where $U_{14,32}$ is given by (8), to give

$$H_{14,32} = (\epsilon_1 - \epsilon_4)\, \delta_{13}\, \delta_{24} + {}^{16}/_{3}\, \alpha_s\, U_{14,32}. \tag{15}$$

It should be noted at this point that the use of the Schroedinger equation to generate the quark and antiquark modes without the addition of spin-spin or spin-orbit terms means that for H^{un} the four p states

$$\{p_{1/2}\bar{p}_{1/2}, p_{1/2}\bar{p}_{3/2}, p_{3/2}\bar{p}_{1/2}, p_{3/2}\bar{p}_{3/2}\}$$

will be degenerate and likewise the four d states

2.4 *The effect* of the non-relativistic approximation on the Hamiltonian

The major effect on the Hamiltonian is brought about by the exclusion of the dynamic interaction *from the* model. As discussed above, both the energy dependent and self-energy terms disappear *from the* Hamiltonian (9) owing to *the dynamic* interaction $\bar{A}$ being zero.

The non-relativisitic Hamiltonian, *after the* exclusion of the energy-*dependent* and self-energy terms, is thus the sum of *an unperturbed* Hamiltonian

$$H^{un}_{14,32} = (\epsilon_1 - \bar{\epsilon}_4)\, \delta_{13}\, \delta_{24} \tag{13}$$

and static interaction Hamiltonian

$$H^{int}_{14,32} = \frac{16}{3}\, \alpha_s\, U_{14,32} \tag{14}$$

where $U_{14,32}$ is given by (8), to give

$$H_{14,32} = (\epsilon_1 - \epsilon_4)\, \delta_{13}\, \delta_{24} + {}^{16}/_{3}\, \alpha_s\, U_{14,32}. \tag{15}$$

It should *be noted* at this point that the use of the Schroedinger equation to generate the quark and antiquark *modes* without the addition of spin-spin or spin-orbit terms means that for H^{un} the four p states

$$(p_{1/2}\bar{p}_{1/2}, p_{1/2}\bar{p}_{3/2}, p_{3/2}\bar{p}_{1/2}, p_{3/2}\bar{p}_{3/2})$$

will be degenerate *and* likewise the four d states

$$(d_{3/2}d_{3/2}, d_{3/2}d_{5/2}, d_{5/2}d_{3/2}, d_{5/2}d_{5/2}).$$

The addition of the interaction term, H^{int}, where the angular momenta of the constituents are coupled to a total angular momentum J, and spin effects are thus included lifts the degeneracy.

The diagrams corresponding to the Hamiltonians(13) and (14) are shown in Fig. 2.2.

2.5 The soft bag

In the literature, the bag is often considered to be a spherical well potential [2], [5], [6]. This means that the quarks and gluons within the bag move as free particles, but cannot extend outside the allotted bag radius R. Viewing the bag as such produces good results. It is, however, possible to soften the bag edge so that the transition from free movement to prohibited motion is not as sharp as is the case in the hard bag. This has been achieved by the use of confining potentials $V \sim r^2$ or r^3 [7]. In this dissertation, we suggest a computationally simple method of mimicking the r^n behaviour using a step function. In addition, we attempt the physically appealing, and novel, idea of treating the gluons in the same soft bag as the quarks.

The simplest way to visualize this is by considering the E.M. analogy introduced in 2.1. For the hard bag, the radial dependence of κ may be viewed as in Fig. 2.3.

Softening of the bag edge would give a dependence similar to that shown in Fig. 2.4.

The main problem of softening the bag lies in choosing the functional form of $\kappa(r)$. Obviously, the form must be realistic, but in addition must be easily soluble computationally. The solution to both these problems is to construct $\kappa(r)$ as a series of steps, as shown in Fig. 2.5.

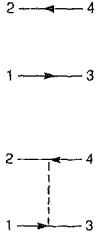

Fig. 2.2: Diagrammatic form of the Hamiltonians(13) and (14) respectively

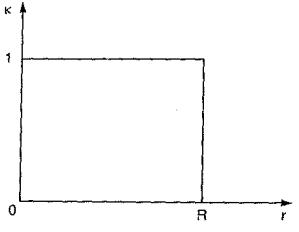

Fig. 2.3: Radial dependence of κ for a hard bag

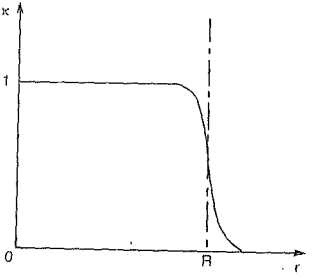

Fig. 2.4: Proposed radial dependence of κ for a soft bag

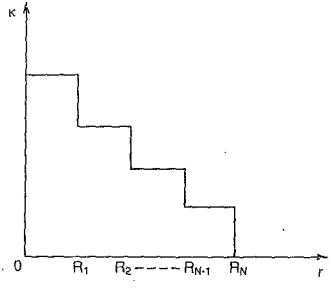

Fig. 2.5 Stepped construction of $\kappa(r)$

The functional form of this dependence is

$$\kappa(r) = \sum_{i=1}^{N} \theta(R_{i-1}, R_i)\ \kappa_i \qquad (16)$$

where $\theta(R_{i-1},R_i)$ = 0 for $r < R_{i-1}$ *or* $r > R_i$
1 for $R_{i-1} \leq r \leq R_i$

and κ_i are chosen to give a suitable profile.

This form of κ can be varied to give different forms of softening by variation of the number of steps, the position of the steps and the magnitudes of the κ_i's.

In the solution of the Schroedinger and Maxwell equations, however, it is the potential that is required. It is clear that the potential must be intimately related to the dielectric constant, but the exact form of the relationship is not obvious. In keeping with the essentially phenomenological formalism of this dissertation, we propose that the relationship is given by

$$V(r) = V_0 \left(\frac{1}{\kappa(r)} - 1\right) \tag{17}$$

where V_0 is a scaling factor which determines the "strength" of the softening process. We propose this equation as a physically plausible relation which is to be understood whatever the form of $\kappa(r)$, continuous or discontinuous. For the proposed multi-stepped form of $\kappa(r)$, it is clear that $V(r)$ has a similar multi-stepped pattern:

$$V(r) = V_0 \sum_{i=1}^{N} \theta\,(R_{i-1}, R_i)\ \left(\frac{1}{\kappa_i} - 1\right). \tag{18}$$

It is this potential that we will use in the following model.

We note at this point that the multistepped form of $V(r)$ in (18) implies the existence of an infinite boundary at some finite radius, which is not

the case for truly soft potentials of the form $V(r) \sim r^2$ or r^3. However, with a suitable choice of the κ_i's, R_i's and V_0, the lower portion of the spectrum and the corresponding wavefunctions produced from (18), should not be too different from that of the genuinely soft bag.

2.5 The quark, antiquark and gluon modes in a soft bag

We turn now to the generation of the modes for the various particles and anti-particles within the bag. The modes are described by equations (10) and (4) for the quarks/antiquarks and gluons respectively. In the case of a spherically symmetric potential, such as is the case in this model, it is possible to separate the variables in the equations so that the wavefunctions $\psi_\ell(\vec{r})$ and $\phi_\ell(\vec{r})$, for quarks/antiquarks and gluons respectively, can be written, without spin dependence, as:

$$\psi(\vec{r}) = \begin{cases} R_\ell(r)\, Y_\ell^m(\Omega) & \text{for quarks} \\ R_\ell(r)\, (-1)^{\ell-m}\, Y_\ell^{-m}(\Omega) & \text{for antiquarks} \end{cases} \qquad (19)$$

$$\phi_\ell(\vec{r}) = \phi_\ell(r)\, Y_\ell^m(\Omega) \text{ for gluons}$$

where $Y_\ell^m(\Omega)$ are the usual spherical harmonics (see [9] for details), and $R_\ell(r)$ and $\phi_\ell(r)$ satisfy the equation

$$\left[\frac{1}{r^2} \frac{d}{dr} \left(r^2 \frac{d}{dr} \right) - \frac{\ell(\ell+1)}{r^2} + k^2(r) \right] F_\ell(r) = 0 \qquad (20)$$

where $F_\ell(r) = R_\ell(kr)$ or $\phi_\ell(kr)$

and $k^2(r) = C(\varepsilon - V(r))$

where ℓ is the orbital angular momentum and

$$C = \begin{cases} 2m/\hbar^2 & \text{for quarks} \\ \hbar c_s & \text{for gluons} \end{cases}$$

It is well known that for a potential of square well form

$$V(r) = \begin{cases} V_0 \text{ for } r<R \text{ where } V_0 \text{ is constant} \\ 0 \text{ for } r>R \end{cases} \qquad (21)$$

the solutions of (20) are given in terms of spherical Bessel and Neuman functions, i.e. $j_\ell(kr)$ and $n_\ell(kr)$, for k(r) real, and modified Bessel and modified Neuman functions $i_\ell(kr)$ and $k_\ell(kr)$, for k(r) imaginary. Thus for a potential of the form (21), the general solution for (20) may be written as

$$F_\ell(r) = Af_\ell(kr) + Bg_\ell(kr) \qquad (22)$$

where $f_\ell(kr) = \begin{cases} j_\ell(Kr) & \text{for } k^2(r) \geq 0 \\ i_\ell(kr) & \text{for } k^2(r) < 0 \end{cases}$

$g_\ell(kr) = \begin{cases} n_\ell(kr) & \text{for } k^2(r) \geq 0 \\ k_\ell(kr) & \text{for } k^2(r) < 0 \end{cases}$

and A and B are constants that have yet to be determined.

At this stage, we consider the multi-step "soft" potential (18). It is clear that the stepping of the potential makes the solution of (20) considerably easier than would have been the case if the potential had been continuous. Instead of being forced to solve for the modes numerically, it is possible to formulate the entire problem analytically. Within each step of the potential, one may write down the solution for (20) analogously to (22). Thus for the ith step, assuming a total of N steps,

$$F^i_\ell(r) = A_i f_\ell(k_i r) + B_i g_\ell(k_i r), \quad i=1 \ldots N \qquad (23)$$

where $k_i^2 = C(\epsilon - V_i)$

with $V_i = V_0 \left(\frac{1}{\kappa_i} - 1\right)$ from (18)

We now impose boundary conditions for the case $F_\ell(r) = R_\ell(r)$, i.e. for the quark/antiquark modes. From the principle of asymptotic freedom, it is clear that κ_1 must be unity, so that $V_1 = 0$. This means that $f_\ell(k_1 r)$ will always be a spherical Bessel function, and $g_\ell(k_1 r)$ a spherical Neuman function. However, we require the wavefunction $R_\ell(r)$ to be finite at $r=0$. Since

$$n_\ell(x) \sim -\frac{(2\ell-1)!}{x^{\ell+1}} \quad \text{for small } x \text{ [7]}$$

it is clear that $n_\ell(x)$ does not remain bounded as $x \to 0$. Thus we must set $B_1=0$, so that

$$R^1_\ell(k_1 r) = A_1 j_\ell(k_1 r), \quad 0 \le r \le R_1. \tag{24}$$

At the *outer* edge of the bag, i.e. $r=R_N$, we require the wave function to be zero:

$$R^N_\ell(k_N R_N) = A_N f_\ell(k_N R_N) + B_N g_\ell(k_N R_N) = 0. \tag{25}$$

Furthermore, at each step edge R_i, we will require the wave function to be logarithmically *continuous*:

$$R^i_\ell(k_i R_{i-1}) = R^{i-1}_\ell(k_{i-1} R_{i-1}), \quad i=2 \ldots\ldots N \tag{26}$$

and $$\frac{dR^i_\ell(k_i R_{i-1})}{dr} = \frac{dR^{i-1}_\ell(k_{i-1} R_{i-1})}{dr}, \quad i=2 \ldots\ldots N.$$

A similar procedure to that described above can be carried out for the gluon modes, i.e. for $F_\ell(r) = \phi_\ell(r)$. The major differences between the two cases are, firstly, the boundary condition imposed on the derivative of the wave function and, secondly, that imposed at $r=R_N$. In the quark case, we have seen that it is sufficient to impose logarithmic continuity of the wave function at the steps in the potential and to enforce nullity on the wave function at $r=R_N$.

Turning to the gluon case, we have stated above our intention to confine the gluons to the same soft bag as the quarks. Since, in our treatment, the gluons behave like photons, we place constraints on the gluon flux $\kappa E_r = \kappa d\phi/dr$, where E_r is the radial component of the colour electric field, in a manner analogous to the electric flux in classical electrostatics. The continuity of the radial electric flux across the interface of two media of different dielectric constants is well known in electrodynamics (see for example [9]). Placing the same constraint on the colour electric field, we thus require continuity of the radial gluon flux across each step in the dielectric constant of the soft bag, expressed by

$$\kappa_i \frac{d}{dr} \phi^i_\ell(k_i R_{i-1}) = \kappa_{i-1} \frac{d}{dr} \phi^{i-1}_\ell(k_{i-1} R_{i-1}), \quad i=2 \ldots\ldots N \qquad (27)$$

Furthermore, at $r=R_N$, i.e. at the outer boundary, the assumption of a colour dia-electric medium surrounding the bag (see section 2.1) means that the radial gluon flux must be zero outside the boundary, as is the case electrostatically with a dia-electric medium. The continuity of the radial gluon flux across the outer boundary must thus imply

$$\kappa_N \frac{d}{dr} \phi^N_\ell (k_N R_N) = 0. \qquad (28)$$

Once we have determined the boundary conditions, it is clear that for an N-step potential, we have a system of 2N-1 equations in the 2N-1 A_i's and B_i's. (We have used the boundary condition at r=0 to eliminate B_1 in both cases.) We may thus set up an equation of the form

$$MX = 0 \qquad (29)$$

where X is a vector of the A_i's and B_i's of dimension 2N-1 and M is a (2N-1) x (2N-1) matrix with entries of the form of f_ℓ's or g_ℓ's and their corresponding derivatives (for quarks/antiquarks) or fluxes (for gluons). We seek non-trivial solutions for X. This is achieved by varying the energy ϵ in the arguments of the f_ℓ's and g_ℓ's until the determinant of M is zero, and then seeking the zero eigenvalue of the resultant constant matrix. The energy ϵ for which this occurs is the eigen energy of the mode. The eigenvectors of this matrix then provide the constants A_i and B_i, and the wave functions can thus be calculated. In all of the above, the f_ℓ's and g_ℓ's and their derivatives are determined using the recursion relations given in [11].

2.7 The vertex integrals $s^{(n)}$ for the soft bag model

The construction of the interaction Hamiltonian (14) requires the calculation of the vertex integrals $s^{(n)}$, given by (8). Once we have solved for the quark/antiquark and gluon modes as described in the previous section, we may set up these integrals as follows:

$$s_{13}^{(n)} = \int \psi_1^*(\vec{r})\, \phi^{(n)}(\vec{r})\, \psi_3(\vec{r})\, d^3r. \tag{30}$$

This integral may be separated into radial and angular parts. The radial part is given by

$$s_{13,\mathrm{rad}}^{(n)} = \int_0^{R_n} R_{\ell,1}(r)\, R_{\ell',3}(r)\, \phi^{(n)}(r)\, r^2 dr. \tag{31}$$

For the soft bag, the radial portion of the integral can be written as

$$s^{(n)}_{13,rad} = \sum_{i=1}^{N} \int_{R_{i-1}}^{R_i} R^i_{\ell,1}(r)\, R^i_{\ell',3}(r)\, \phi^{(n)}(r)\, r^2 dr \qquad (32)$$

with $R_0 = 0$,

and thus consists of integrals over products of three Bessel, Neuman, modified Bessel or modified Neuman functions. These are computed numerically.

The angular part can be done analytically. The derivation given in the previous section produces angular wave functions for the quark and antiquark modes which are simply spherical harmonics $Y^m_\ell(\Omega)$. These take no account of the spin wave function. To include the spin contribution, we can make use of the expression for the angular portion of the $s^{(n)}$ integrals derived for the relativistic case in [12]:

$$s^{(n)}_{13,ang} = (-1)^{m_3+\frac{1}{2}} \frac{\hat{J}_1 \hat{J}_3 \hat{\Lambda}}{\sqrt{4\pi}} \begin{pmatrix} J_3 & \Lambda & J_1 \\ -m_3 & m & m_1 \end{pmatrix} \begin{Bmatrix} J_3 & \Lambda & J_1 \\ \frac{1}{2} & 0 & \frac{1}{2} \end{Bmatrix}$$

$$\times \left[\frac{1 + (-1)^{\frac{\ell_1 + \ell_3 + \Lambda}{2}}}{2} \right] \qquad (33)$$

where J_1 = the total angular momentum of the state,

Λ = orbital angular momentum of gluon,

m_1 = projection of J_1,

and $\hat{J}_1 = \sqrt{2J_1+1}$

The last term in (33) determines the parity selection rules while the other terms govern the angular momentum selection.

2.8 The coupling of the angular momenta

The interaction term $U_{14,32}$ is given by (8). Once the $s^{(n)}$ integrals have been carried out, it is necessary to couple the angular momenta of the input and output states to the total angular momentum of the meson J.

For both the J/ψ and Υ meson, J=1. The full expression for the coupling, which includes the angular portions of the $s^{(n)}$ integrals, is

$$W = (-1)^{J_1+J_3+J_1} \hat{J}_1 \hat{J}_2 \hat{J}_3 \hat{J}_4 (\hat{\Lambda})^2 \begin{Bmatrix} J_2 & J_3 & J \\ J_1 & J_4 & \Lambda \end{Bmatrix}$$

$$\times \begin{pmatrix} J_3 & \Lambda & J_1 \\ \frac{1}{2} & 0 & -\frac{1}{2} \end{pmatrix} \begin{pmatrix} J_4 & \Lambda & J_2 \\ \frac{1}{2} & 0 & -\frac{1}{2} \end{pmatrix} \left[\frac{1+(-1)}{2}^{\ell_1+\ell_3+\Lambda}\right] \left[\frac{1+(-1)}{2}^{\ell_2+\ell_4+\Lambda}\right]. \qquad (34)$$

Details of the coupling of the angular momenta can be found in [10]. We are now in a position to write the interaction $U_{14,32}$ as

$$U_{14,32} = \sum_{n\neq 0} \frac{s^{(n)}_{13,rad}\, s^{(n)}_{24,rad}\, W}{(\omega^L_n)^2} \qquad (35)$$

where ω^L_n is the gluon eigen energy for the nth state.

3. THE STATES FOR J/ψ AND ϒ MESONS

In this chapter, we apply the formalism of the soft bag to the $J^P = 1^-$ states for the J/ψ and ϒ mesons. We should obtain a reasonable fit on the grounds that the non-relativistic approximation is expected to be valid for the heavy c and b quarks which make up these mesons.

3.1 The parameters for the model

We have three parameters that may be used to fit the data. These are the extent of the confining potential R_N, the coupling constant α_s, and the mass scaling factor β, introduced above. All of these parameters have, in theory, unlimited ranges, but limits are imposed by the desire to obtain reasonable agreement with results obtained both from other theories and experiment. We thus hope to obtain final parameters within the following bounds:

$$\begin{aligned} &0 < \alpha_s \leq 2.0 \\ &R_N \sim 1 \text{ fm} \\ &\beta_c \sim 2 \text{ GeV.fm (for J/ψ)} \\ &\beta_b \sim 5 \text{ GeV.fm (for ϒ)}. \end{aligned} \tag{35}$$

The last condition should allow us to obtain values for the mass of the c quark of between 1.6 and 2.0 GeV and values of between 4.5 and 5.5 GeV for the mass of the b quark.

Of the three conditions in (36), the limit on α_s is the weakest. There is very little to guide us in our choice of α_s, other than the desire that it should be "small", i.e. the deviations from the unperturbed states should not be enormous.

It should be noted that R_N is not the size of the meson. Once the states have been determined, a RMS radius of the meson can be calculated, which gives a more realistic estimate of the meson's size. R_N is used to set the energy scale of the meson spectrum. The original M.I.T. bag[1] does not use the radius as a parameter, but rather fixes it using the quadratic boundary condition[8]. However, the vacuum pressure B used in the M.I.T. bag fulfills the same role of overall scaling there as the radius R_N does in our case.

3.2 The method of fitting the data

The data are fitted using the same procedure as that used in [5] and [6]. The single particle modes are generated using a radius of 1 fm. These modes are then substituted in (13) and (14) to obtain $H^{un}{}_{14,32}$ and $H^{int}{}_{14,32}$. The value of α_s is then varied and the meson states calculated for each value of α_s. The choice of α_s is determined as follows:

Consider a measured spectrum T_i and a calculated spectrum E_i. We choose α_s such that

$$\left.\frac{E_2}{E_1}\right|_{\alpha_s} = \frac{T_2}{T_1} \,. \tag{37}$$

This value of α_s is then used in the $H_{14,32}$ matrix to generate the wave functions for the meson states.

Once the α_s has been fixed, we scale the whole spectrum using the radius R_N. The parameterization (11) of the mass means that the eigenvalues E_i scale like the mass, i.e. like the inverse of the radius. We thus choose R_N so that

$$\frac{E_1}{R_N} = T_1 \,. \tag{38}$$

This value of R_N is then used to scale the whole spectrum, so that a new spectrum E'_i is obtained such that

$$E'_i = \frac{E_i}{R_N} \qquad \text{for all } i. \tag{39}$$

The fitting of the mass scaling parameter β is more difficult. Both α_s and R_N can be fitted once the single particle modes and the Hamiltonians H^{un} and H^{int} have been determined. On the other hand, the quark and anti-quark modes depend intimately on the value of β. Thus each value of β requires the generation of the modes and Hamiltonians. This is computationally tedious, and so results are calculated for a few values of β only. This is not viewed as a severe limitation, as we expect the theory to be reasonably independent of the mass scaling.

A comment is in order at this point concerning the accuracy of the method of fitting the parameters described above. It is possible to obtain

better overall fits by using, for example, a least squares method. However, the essentially approximate and phenomenological nature of the model means that the additional work required by such a method is out of all proportion to the actual improvement shown in the final results. In addition, using such a minimization scheme might well hide trends and shortcomings in the model which show through more clearly with a simple fitting mechanism.

It is also worth noting at this stage that the coupling constant α_s is theoretically flavour-independent[16]. It would thus be very gratifying to show that the same coupling can be used for both c and b quarks without the use of unrealistic values for R_N and β for one or other of the quark flavours.

3.3 The choice of the confining potential

Before we calculate the single quark/anti-quark and gluon modes, we must choose the form of the bag with which we obtain confinement. In Section 2.5 we postulated a general form of the potential which required a choice of values for the steps in the dielectric constant κ as well as the positions of these steps, and a constant potential "strength" factor V_0. We now propose values for these parameters.

We are free to choose any values we like for the parameters of the potential, within the very weak and subjective constraint of realism. However, the success of the bag model using a hard-walled potential means that we should consider only reasonably small perturbations of this form.

As we noted in Chapter 1, we are attempting to mimic the ν^n bag used in the literature. To this end, we choose values of κ that will give a potential that rises at least as fast as the harmonic oscillator potential. The number of steps is still an open choice. Clearly, the more steps we use, the more we may refine the potential, but at the cost of increased computation time. For this dissertation, we have chosen a 4-step κ function. Values chosen for this function are given with their corresponding positions in Table 3.1.

Table 3.1 Step positions and values of κ

Step number (i)	Position (R_i)	Magnitude (κ_i)
1	0.25	1
2	0.50	0.9
3	0.75	0.75
4	1.00	0.57

These values should be viewed in conjunction with Figure 2.3.

The choice of the last step position R_4 is arbitrary at this stage. Since we are going to scale the final values by the radius R_4, we can take R_4 to be 1 for convenience in the calculations. This will provide results in units of $1/R$, which can then be scaled using the procedure of Section 3.2 to provide the final radius.

The only parameter remaining to completely determine the potential is the softening strength V_0. The choice of this parameter is determined by the desire to have all the modes used within the affected area. It is simple to calculate the energies of states for a square well, since the zeros of the Bessel functions are well known. The lowest d-state energy, which is the highest used in this model, is of the order of 300 MeV. Since the softening of the bag will increase this value, we would like the final potential step V_4 to be of the order of 1 GeV. This we achieve by setting V_0 to a value of 1.5 GeV.

The resultant potential can be calculated from (18). The values are given in Table 3.2 for the same positions as for κ in Table 3.1.

Table 3.2 Step positions and values for the confining potential V

Step Number (i)	Position (R_i)	Magnitude (V_i)
1	0.25	0
2	0.50	0.167
3	0.75	0.500
4	1.00	1.132

The potential function V is shown in Figure 3.1.

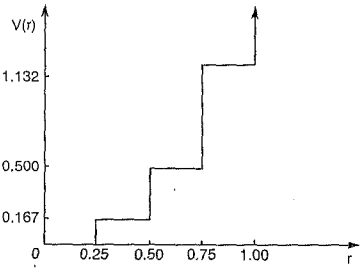

Fig. 3.1: The chosen confining potential $V(r)$

We use the same potential for both the J/ψ and Υ systems. The consequences of this choice will be discussed later.

3.4 The single quark/antiquark states

The single quark/antiquark states for the soft bag are calculated using the procedure described in Section 2.6 above. We include only the lowest five single particle states ($s_{1/2}, p_{1/2}, p_{3/2}, d_{3/2}, d_{5/2}$). Taking higher states into account has little influence on the collective modes. This is in line with our tacit assumption that the Schroedinger energy ϵ is small compared to the total energy of the quark $\epsilon + m_0c_s^2$, in keeping with the assumption of non-relativistic quark behaviour. It is clear that we have to view the Schroedinger energy as a correction to the

rest energy of the quark. We note that, due to the lack of spin effects in the Schroedinger equation, the $p_{1/2}$ and $p_{3/2}$ single particle states are degenerate, as are the $d_{3/2}$ and $d_{5/2}$ states.

We calculate the single particle states for three values of the mass scaling β; viz. 1.8, 2.0, 2.2 GeVfm for the J/ψ and 4.2, 4.5, 5.0 GeVfm for the T. Values obtained from these calculations using the potential of Section 3.3 are tabulated in Table 3.3 for the J/ψ and Table 3.4 for the T.

Table 3.3: Single quark/antiquark energies for the J/ψ meson for the potential of Table 3.2. Energies are in GeV

mode	β 1.8	2.0	2.2
s	0.348	0.327	0.312
p	0.591	0.556	0.530
d	0.840	0.794	0.754

Table 3.4: Single quark/antiquark energies for the Υ meson for the potential of Table 3.2. Energies are in GeV

mode	β 4.2	4.5	5.0
s	0.221	0.211	0.201
p	0.378	0.368	0.348
d	0.536	0.515	0.490

We also provide, for comparison, values for the same range of β for a hard bag. These values are tabulated in Table 3.5 for the J/ψ and Table 3.6 for the Υ.

Table 3.5: Single quark/antiquark energies for the J/ψ meson for a hard bag. Energies are in GeV

mode	β 1.8	2.0	2.2
s	0.109	0.094	0.089
p	0.221	0.195	0.180
d	0.358	0.322	0.292

Table 3.6: Single quark/antiquark energies for the Υ meson for a hard bag. Energies are in GeV

mode	β 4.2	4.5	5.0
s	0.048	0.043	0.038
p	0.094	0.089	0.079
d	0.155	0.145	0.129

The effect of the softening on the modes can clearly be seen by comparing Tables 3.3 and 3.5 and Tables 3.4 and 3.6. All the modes are shifted upwards by the potential, as would be expected. The Υ modes are affected to a greater degree than the J/ψ modes due to the fact that they lie lower in the bag. This implies that they "see" the potential more strongly than the J/ψ modes do. In both cases the shift is larger for the p and d states than for the s states, as we expected. There is no re-ordering of the states.

The modes are normalised so that

$$\int |\psi(\mathbf{r})|^2 \, d^3r = 1. \tag{40}$$

Since the $Y_\ell^m(\Omega)$ are normalised, we need only ensure that

$$\int_0^{R_N} [R(r)]^2 \, r^2 dr = 1. \tag{41}$$

3.5 The gluon states

The gluon modes for the soft bag are determined in a similar manner to the single quark/antiquark states, also using the procedure of Section 2.6. We include a total of nineteen longitudinal gluon states, up to the 5p, in the calculation. The higher energy states contribute very little to the $U_{14,32}$ term. This is due to both the oscillatory nature of the wave functions, which decreases the $s^{(n)}$ integrals, and the factor $(\omega_n^L)^2$ under the limit in (35), which together ensure that the sum over the gluon modes converges rapidly. The gluon modes are calculated using the parameters for κ given in Table 3.1. Values for the lowest few modes are given in Table 3.7.

Table 3.7: Gluon modes for κ as in Table 3.1

Mode	Energy (GeV)
1s	0.669
1p	1.044
2s	1.360
1d	1.445
2p	1.695
1f	1.770

For comparison, the same gluon modes for a hard bag are given in Table 3.8

Table 3.8: Gluon modes in a hard bag

Mode	Energy (GeV)
1s	0.889
1p	0.413
2s	1.530
1d	0.663
2p	1.174
1f	0.894

From Tables 3.5 and 3.6 it is clear that the gluon modes are drastically affected when the bag is softened. This is due to the boundary condition of continuous flux across a step boundary. The modes with $\ell \neq 0$ are affected to a much greater extent than the s modes which results in a re-ordering of the modes. This is in contrast to the quark case above, where the mode order remains the same.

It should be noted that the gluon modes are generally larger than the quark/antiquark modes. This is in contrast to the relativistic case [6], where for u and d quarks, the quark states are of comparable energy to the gluon states. The higher gluon energies once more justify the use of a static approximation, as they render the dynamic contribution unimportant. This is the opposite of the case in [6].

The gluon modes are normalised in a similar fashion to the quark modes:

$$\int_0^{R_N} [\phi(r)]^2 \; r^2 dr = 1. \qquad (42)$$

3.6 The calculation of the interaction term $U_{14,32}$

Once the modes have been determined, we can calculate the interaction term $U_{14,32}$ using (35). The radial $s^{(n)}$ integrals are calculated using a fifty point Simpson routine. The coupling factor W (34) is calculated using a standard routine for the 6-J coefficients and the packed storage method [11] for the 9-J coefficients to save memory space during computations.

3.7 The J/ψ spectrum

Once we have determined the single particle states and calculated the interaction term $U_{14,32}$ it is a simple matter to diagonalize the Hamiltonian $H_{14,32}$ given by (15). We do this for various values of the coupling constant α_s. The diagonalization yields both the energies and wave functions of the meson states.

In this model we obtain a 9-dimensional $H_{14,32}$. We use the following $|q\bar{q}\rangle$ states in the calculations:

$$|s_{1/2}\bar{s}_{1/2}\rangle,\ |p_{1/2}\bar{p}_{1/2}\rangle,\ |p_{3/2}\bar{p}_{1/2}\rangle,\ |p_{1/2}\bar{p}_{3/2}\rangle,\ |p_{3/2}\bar{p}_{3/2}\rangle,$$

$$|d_{3/2}\bar{d}_{3/2}\rangle,\ |d_{5/2},\ \bar{d}_{3/2}\rangle,\ |d_{3/2}\bar{d}_{5/2}\rangle,\ |d_{5/2}\bar{d}_{5/2}\rangle.$$

We thus determine the lowest nine $J^P=1^-$ states for the J/ψ. Only six such states are known at present. While we find nine states, our model can in any case only possibly describe some lower states. For the higher states the model is surely insufficient without a knowledge of how to calculate decays and corresponding widths.

We provide results in Table 3.9 for the lowest nine states for the same values of β used in Section 3.4, viz. β = 1.8, 2.0 and 2.2. GeVfm for the potential of Section 3.3. We also provide data for a hard bag for the case β = 1.8 GeVfm. The experimental results are shown in Table 3.10, and are taken from [15]. For each set of calculated data, the value of α_s used is also given.

Table 3.9: J/ψ states for various β, for the potential of Table 3.2 and for a hard bag. Energies in GeV. Underlining indicates input

β = 1.8	β = 2.0	β = 2.2	β = 1.8 (hard bag)
α_s = 1.00	α_s = 1.19	α_s = 2.59	α_s = 0.8
3.1	3.1	3.1	3.1
3.687	3.684	3.682	3.683
3.840	3.861	4.117	3.945
3.910	3.935	4.264	4.065
3.991	4.038	4.554	4.199
4.324	4.297	4.609	4.345
4.352	4.330	4.731	4.514
4.406	4.394	4.906	4.561
4.449	4.440	4.992	4.720

Table 3.10: Experimental J/ψ states from [15].

State	Energy (GeV)	Width (GeV)
1	3.097	$6.3.10^{-5}$
2	3.686	$2.15.10^{-4}$
3	3.770	0.025
4	4.030	0.052
5	4.159	0.078
6	4.415	0.043

From the data given in Tables 3.9 and 3.10, we see that the best calculated data are those for β = 2.0 GeVfm. These data give results that are within 3% of the experimental data for all the tabulated states. The higher states are consistently lower. However, in view of the crudity of the model, the agreement, even for the higher states, is surprisingly good. We also note that the data for β = 2.2 GeVfm are in poor agreement with the measured data, deviations being up to 10% for the third and fifth states. In addition, it can be seen that the soft bag offers some improvements over the hard bag for the lower states, in particular the ψ (3770) where the soft bag model yields a value only 1,8% above the experimental result, while the hard bag calculation is 4,6% above the experimental observation. For the higher states, the simplicity of the model means that a comparison would not be too meaningful.

We also note that the value of α_s which corresponds to the best mass scaling $\beta = 2.0$ GeVfm, is $\alpha_s = 1.19$. While this value is higher than the values given in [5] and [6], it is still reasonable. We note that Heiss and Quick[5] obtain $\alpha_s = 0.38$, while Gering[6] has $\alpha_s = 0.757$. These differences occur owing to the use of different light meson states to obtain the fit. In the light of this it is thus not surprising that the use of heavy quarks gives rise to a somewhat different coupling constant than that obtained by the use of light quarks. We find it rather satisfying that we remain in the same order of magnitude.

As can be seen from 3.9, we predict three states at higher energies than those observed rimentally. These three states lie at 4.330 GeV, 4.394 GeV and 4.440 GeV. Assuming a 3% error, which is consistent with the remainder of this calculated spectrum, we obtain values of 4.460 GeV, 4.526 GeV and 4.573 GeV. (We have assumed the model calculations to be low on the basis of the values for the $\psi(4030)$, $\psi(4160)$ and $\psi(4415)$). The identification of these states in spectroscopic $^{2S+1}L_J$ notation is not possible in the bag model, as we have J as a good quantum number but not L. This is in contrast to the potential models, where we have both J and L as good quantum numbers, and such identification is possible. In addition, these states all lie above the charm threshold of 3.73 GeV, so that in a potential model they may be considered to be mixtures of $^3S_1$ and $^3D_1$ states rather than pure states.

On the other hand, in the light of the bunching of the higher states, we suggest, albeit cautiously, that certain of these states overlap. It is known from experiment that the ψ states that lie above the charm threshold have fairly broad widths.

We also note that the value of α_s which corresponds to the best mass scaling β = 2.0 GeVfm, is α_s = 1.19. While this value is higher than the values given in [5] and [6], it is still reasonable. We note that Heiss and Quick[5] obtain α_s = 0.38, while Gering[6] has α_s = 0.757. These differences occur owing to the use of different light meson states to obtain the fit. In the light of this it is thus not surprising that the use of heavy quarks gives rise to a somewhat different coupling constant than that obtained by the use of light quarks. We find it rather satisfying that we remain in the same order of magnitude.

As can be seen from Table 3.9, we predict three states at higher energies than those observed experimentally. These three states lie at 4.330 GeV, 4.394 GeV and 4.440 GeV (assuming a 3% error, which is consistent with the remainder of this calculated spectrum, we obtain values of 4.460 GeV, 4.526 GeV and 4.573 GeV). We have assumed the model calculations to be low on the basis of the values for the $\psi(4030)$, $\psi(4160)$ and $\psi(4415)$. The identification of these states in spectroscopic $^{2S+1}L_J$ notation is not possible in the bag model, as we have J as a good quantum number but not L. This is in contrast to the potential models, where we have both J and L as good quantum numbers, and such identification is possible. In addition, these states all lie above the charm threshold of 3.73 GeV, so that in a potential model they may be considered to be mixtures of $^3S_1$ and $^3D_1$ states rather than pure states.

On the other hand, in the light of the bunching of the higher states, we suggest, albeit cautiously, that certain of these states overlap. It is known from experiment that the ψ states that lie above the charm threshold have fairly broad widths.

We propose that, for example, the calculated ψ (3935) and ψ (4038) may both be identified with the experimental ψ (4030), as unresolved states within the experimental peak. The same suggestion can be made for the calculated ψ (4297) and ψ (4330) {identified with the experimental ψ (4160)} and for the calculated ψ (4394) and ψ (4440) {identified with the experimental ψ (4415)}. We must state, however, that this is speculative, as the non-relativistic model used does not allow us to predict the widths of the states, which appear as infinitely stable modes. Owing to the lack of further information, a more quantitative statement on this matter is not possible.

Alternatively, the grouping of the states may be due to the lack of a spin-dependent term in the radial portion of the Hamiltonian. The inclusion of such a term may increase the splitting of these states and resolve the near-degeneracy of the states. This explanation is probably more likely than the overlapping of the higher states.

3.8 The T spectrum

We calculate the T spectrum in a similar manner to the J/ψ. We use the same confining potential for the T as for the J/ψ. We again calculate only $J^P = 1^-$ states, and use the same $|q\bar{q}>$ states as for the J/ψ.

We thus predict nine T states, as was the case for the J/ψ. Only six T states have been observed experimentally at this stage [16]. Again, the lack of good L means that identification of the states is not possible, and the comments made in the previous section concerning states above the charm threshold in the case of the J/ψ apply here to states above the bottom threshold of 10.56 GeV.

We provide calculated results in Table 3.11 and experimental data in Table 3.12. In Table 3.12, we also include values for two predicted states as calculated by Quigg[16] using a potential model. These results are close to those obtained by other models, notably [20] and [21], and so provide a reasonable basis for comparison. We provide results for β = 4.2, 4.5 and 5.0 GeVfm. We also quote the α_s value used, as for the J/ψ.

Table 3.11: T states for various β, for the potential of Table 3.2. Underlining indicates input. Energies in GeV

β = 4.2	β = 4.5	β = 5.0
α_s = 2.00	α_s = 0.98	α_s = 2.94
9.460	9.460	9.460
10.024	10.023	10.025
10.374	10.174	10.361
10.434	10.237	10.385
10.551	10.333	10.613
10.725	10.558	10.839
10.726	10.585	10.874
10.820	10.641	11.063
10.957	10.680	11.227

Unlike the situation with the J/ψ, none of the calculated spectra are appreciably more accurate than the others. For the states below threshold, β = 4.5 GeVfm yields the best results, being accurate to within 1% of the measured data. The small value of α_s for β = 4.5 GeVfm is also pleasing.

Above threshold, β = 5.0 GeVfm gives the closest fit, except for T (10578) where β = 4.5 GeVfm is still better. The high value of α_s necessary to obtain this fit does, however, give cause for concern. We thus conclude that β = 4.5 GeVfm is probably the best spectrum to use for future comparisons. β = 4.2 GeVfm does not provide particularly noteworthy results either above or below threshold.

We predict only one excited state for the T. For β = 4.5 GeVfm, this state is obviously too low, so we use the β = 5.0 GeVfm spectrum and predict a state of 11.227 GeV.

Table 3.12: Experimental T states from [16]

State	Energy (GeV)	Width (GeV)
1	9.460	$4.3.10^{-5}$
2	10.023	$3.0.10^{-5}$
3*	10.149	-
4	10.356	$2.6.10^{-5}$
5*	10.434	-
6	10.578	0.024
7	10.865	0.11
8	11.019	0.079

* Predicted state [16] included for comparison.

Above threshold, β = 5.0 GeVfm gives the closest fit, *except for* T (10578) where β = 4.5 GeVfm is still better. The high value of α_s necessary to obtain this fit does, however, *give cause* for concern. We thus conclude that β = 4.5 GeVfm is probably the best spectrum to use for future comparisons. β = 4.2 GeVfm does not provide particularly noteworthy results either above or below threshold.

We predict *only one* excited state for the T. For β = 4.5 GeVfm, this state is obviously too low, so we use the β = 5.0 GeVfm spectrum and predict a state of 11.227 GeV.

Table 3.12: *Experimental T states from* [16]

State	Energy (GeV)	Width (GeV)
1	9.460	$4.3.10^{-5}$
2	10.023	$3.0.10^{-5}$
3*	10.149	-
4	10.356	$2.6.10^{-5}$
5*	10.434	-
6	10.578	0.024
7	10.865	0.11
8	11.019	0.079

* Predicted state [16] included for comparison.

As in the J/ψ case, we may make the cautious suggestion of overlapping states above threshold. In all three calculated spectra, the four states above threshold can be formed into two pairs which have differences close to the measured widths for the Υ (10578) and Υ (10865) states (Table 3.12). As was noted for the J/ψ, however, the non-relativistic bag model does not allow further investigation. Once again, however, the lack of spin dependence in the radial Hamiltonian is viewed as the more satisfactory explanation for the bunching of the higher states.

We now consider the effect of using the same confining potential for the J/ψ and the Υ. We have seen above that none of the three spectra provide entirely satisfactory results for the whole range of available experimental data. It may be possible to improve the spectra by changing the form of the potential. In the case of $\beta = 4.5$ GeV/fm, a potential that is more constricting at higher energies would cause the higher $q\bar{q}$ modes to increase in energy, which may improve the fit above threshold. The form of the potential also affects the RMS radii of the states. Further comments on the modification of the potential in this regard for Υ systems may be found in the next section. The phenomenological nature of the soft bag model, however, allows us considerable freedom in the choice of parameters for the potential, and "fine tuning" is possible, although physically not too sensible.

3.9 The RMS radii of the mesons and the quark masses

The calculation of the meson spectra is carried out with R_N set to unity, for ease of calculation, and to obtain values that scale as $1/R_N$. Once the spectrum for a particular meson has been determined, the scaling procedure of Section 3.2, in particular Equation (38), provides us with the actual value of R_N.

It is not surprising to find that the extent of the bag R_N is not flavour independent. It has been determined, both by the use of potential models [16] and experiment [17], that the Υ meson is more deeply bound (in the terminology of potential models) than the J/ψ. This implies that the RMS radius of the Υ is less than that of the J/ψ. In the bag picture, we thus expect the Υ to be smaller than the J/ψ bag.

The soft bag model yields R_N values of 1.147 fm for the J/ψ and 0.91 fm for the Υ, for the best fit values of $\beta = 2.0$ GeV/fm and $\beta = 4.5$ GeV/fm respectively. These values are in accordance with expectations for heavy quark mesons, since they agree well with the values for R_N obtained for a hard bag in [5] (0.7 fm) and [6] (0.923 fm) for light mesons.

Once we have determined R_N, we may calculate the RMS radius for each state in the spectrum. The RMS radius of the jth state is given by

$$\sqrt{\langle r^2 \rangle_j} = \left(\sum_{i=1}^{9} c_{ij}^2 \langle 1 | r^2 | 1 \rangle \right)^{\frac{1}{2}}. \qquad (43)$$

There are no cross terms due to the lack of mixed $|q\bar{q}\rangle$ states in this model.

Equation (43) is solved using a Simpson's Rule integration over the normalised quark radial wave functions; the c_{ij} are given by the diagonalization procedure, and are already normalized so that

$$\sum_{i=1}^{9} c_{ij}^2 = 1. \qquad (44)$$

We list values for $\langle r^2 \rangle$ for the J/ψ (β = 2.0 GeVfm) in Table 3.13 for the Υ (β = 4.5 GeVfm) in Table 3.14.

Table 3.13: RMS radii for the J/ψ spectrum

State	RMS radius (fm)
1	0.420
2	0.535
3	0.535
4	0.537
5	0.539
6	0.602
7	0.601
8	0.600
9	0.602

We first examine the RMS radii for the J/ψ. The radius of the ground state (state 1 in Table 3.1) agrees well with the experimental value in [17]. However, the radii of the excited states are too small. The reason for this is found in the use of an infinite well type of potential [6]. For this case the potential increases too fast for the higher modes. A more gently increasing potential, such as a power law potential, would give larger radii for the excited states.

Table 3.14: RMS radii for the Υ spectrum

State	RMS radius (fm)
1	0.495
2	0.626
3	0.627
4	0.629
5	0.623
6	0.678
7	0.677
8	0.676
9	0.678

Turning now to the Υ radii, we see that the agreement with experiment [17] is poor. The ground state radius is too large and the excited states' radii are too small. The explanation for the latter is the same as that for the J/ψ excited states. The former requires a different explanation, which can be found in the choice of the potential in this dissertation. We have already noted above that the Υ, in terms of a potential model, is more deeply bound than the J/ψ. This means that the softening should extend further into the Υ bag than into the J/ψ bag. The choice made in this model is sufficiently narrow for the J/ψ, but is still too broad for the Υ. This can be corrected by a different choice of the step position in the dielectric constant for the Υ bag to "squeeze" the lower states of the Υ.

In addition to allowing us to calculate RMS radii for the meson states, knowledge of R_N places us in a position to fit the free quark masses using the parameter β and equation (11'. We have seen that the best fits for the J/ψ are obtained for β = 2.0 GeVfm and for 4.5 GeVfm for the T. With the corresponding R_N values for these spectra being 1.147 fm and 0.91 fm respectively, we obtain:

$$m_c = 1.74 \text{ GeV} \quad \text{and}$$
$$m_b = 4.94 \text{ GeV}$$

Both these values are within the expected limits, and agree well with literature values [1], [16], [18], [19], [26], [28].

3.10 Comparison of the soft bag model with potential models

As we noted in Chapter 1, the most popular approach to theoretical heavy quark spectroscopy has been that of potential models. There have been many different potentials proposed for $q\bar{q}$ systems (see [18] → [28] for examples) which differ in the number and type of terms included in the Hamiltonian as well as the functional form of the confining/ interaction potential. The majority use either a close range coulombic potential matched to a long-range power law term [27], or a universal power law potential of the form [26]

$$V(r) = A + Br^{\alpha} + \text{spin dependent terms}$$

with α - 0.1. Various forms of spin dependence are used. In some cases ([21], [23], [25]) the spin is included explicity in V, while in others ([26], [27]), spin averaged wave functions are used. Both these potentials are used in a flavour independent manner, and spectra are usually produced for both J/ψ and T systems.

The results obtained for the J/ψ using the soft bag model are compared with those obtained using both the above groups of potential models. We give the spectra in Fig. 3.2 for power law models [19], [21], [27] and in Fig. 3.3 for coulomb + power law models [22], [23], [25].

The spectra show clearly that the soft bag model produces a J/ψ spectrum that is comparable in accuracy to that of the potential model. The main deficiencies appear to be for the higher states, although we note that the predicted ψ (4460) state is close to Richardson's predicted ψ (4498) [22]. These deficiencies could possibly be corrected by expanding the 'bowl' of the potential, i.e. moving the infinite edge to a larger radius and accordingly extending the steps. This would expand the region within which the stepped potential gives results close to those of a $V(r) \sim r^n$ type of bag.

We now turn our attention to the T spectrum. Owing to the non-relativistic character of the $b\bar{b}$ system, the T meson is easily modelled using a potential and solving the Schroedinger equation. Once again, there are many published results, and we quote only a representative group for the power law, and the coulomb + power law models. The former are shown graphically in Fig. 3.4, with results from [21] and [27], and the latter in Fig. 3.5, with results from [20], [22] and [25], together with soft bag results.

Figure 3.2

Experimental, soft bag and power law potential model results

for the J/ψ meson spectrum

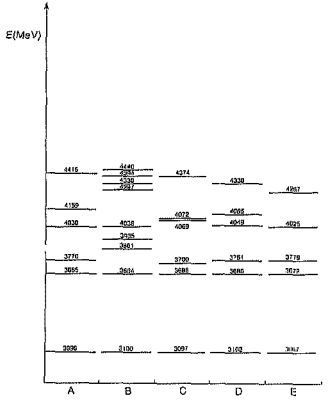

A: Experimental ([16])

B: *Soft bag mode*)

C: Portilho and Shokranian ([19])

D: Stanley and Robson ([21])

E: Barik and Jena ([27])

Figure 3.3

Experimental, soft bag and coulomb + power law potential model results for the J/ψ meson spectrum

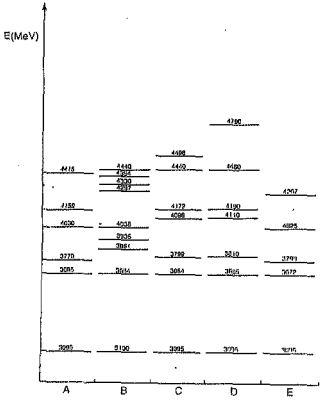

A: Experimental ([16])

B: Soft bag model

C: Richardson ([22])

D: Eichten et al. ([23])

E: Dias de Deus ([25])

Figure 3.4

Experimental, soft bag and power law potential model results for the T meson spectrum

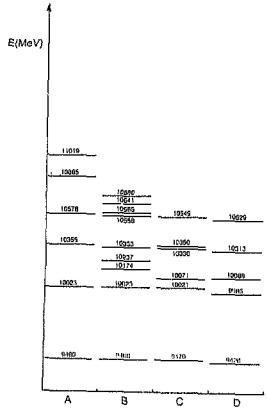

A: *Experimental* ([16])

B: Soft bag model

C: Stanley and Robson ([21])

D: Barik and Jena ([27])

Figure 3.5

Experimental, soft bag and coulomb + power law potential model results for the T meson spectrums

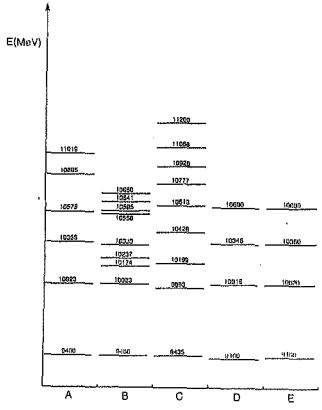

A: Experimental ([16])

B: Soft bag model

C: Kulshreshtha and Kaushal ([20])

D: Richardson ([22])

E: Dias de Deus ([25])

As in the case of the J/ψ, the soft bag results are of an accuracy comparable to that of the predictions of the potential models, although the higher states are low for $\beta = 4.5$ GeVfm as noted in Section 3.8. This can probably be corrected by modification of the bag in a similar fashion to that suggested for the J/ψ. On the other hand, it is gratifying to note that the two lower predicted states (T (10174) and T (10333) in the soft bag model) lie close to the potential model predictions for these states (T (10200) and T (10500) [23], T (10149) and T (10434) [16], T (10137) and T (10421) [22], and T (10285) [24]).

3.11 The meson wave functions in the soft bag model

In addition to calculating the meson spectra, we are also able to calculate the wave functions in terms of their components in the expansion

$$\psi(\vec{r}) = \sum_i c_i \psi_i(\vec{r}) \qquad (43)$$

where $\psi_i(\vec{r})$ is the wavefunction for a particular $|q\bar{q}\rangle$ mode. Since we have a total of nine $|q\bar{q}\rangle$ states, we have nine components to each wave function. We list the wave functions corresponding to the nine calculated states in Appendix A for $\beta = 2.0$ GeVfm for the J/ψ, and $\beta = 4.5$ GeVfm in the case of the T.

The wave functions for both the J/ψ and the T follow expectations in that the lowest state is predominantly $|s_{1/2}\bar{s}_{1/2}\rangle$, whereas the upper states have significant mixing of modes. In both cases, however, we have the appearance of what we will term exclusive coupling, where certain states have strong components of certain $|q\bar{q}\rangle$ modes, and zero components for all others. For both the J/ψ and T, the fourth and seventh

wavefunctions are exclusive couplings of $|p_{1/2}\bar{p}_{3/2}\rangle$, $|p_{3/2}\bar{p}_{1/2}\rangle$, $|d_{3/2}\bar{d}_{5/2}\rangle$ and $|d_{5/2}\bar{d}_{3/2}\rangle$. In all of the above cases, the two $|p_i\bar{p}_j\rangle$ components are equal and likewise the two $|d_i\bar{d}_j\rangle$ components, although it is to be expected from the symmetry of the pairs, and occurs for all the meson states.

Examining the J/ψ case first, we further note that the d components of the seventh state are equal to the p components of the fourth, and the p components of the seventh state are equal to the d components of the fourth, apart from a change of sign. The same situation occurs for the fourth and seventh states of the T spectrum, except that the sign change occurs for the d-components of the seventh state and the p-components of the fourth.

It seems highly probable that this exclusive coupling is simply a spuriosity of the model used in this dissertation, in particular the degeneracy of the p and d states at $\alpha_s=0$ and the spin independence of the interaction. We thus do not believe this phenomenon to be of particular physical relevance.

4. CONCLUSIONS

The bag model is generally accepted as a good phenomenological theory of the structure of quark systems, but has been applied mainly to light quark systems. In this dissertation, we show that the bag model can be used to provide an accurate description of the $J^P = 1^-$ states of the J/ψ and Υ mesons. This means that the bag model is consistent, and makes it more acceptable as a general descriptive model of quark system spectroscopy.

In calculating the meson spectra, we make use of a non-relativistic approximation for the quark systems. We thus use the Schroedinger rather than the Dirac equation for the single quark modes. This is valid owing to the heavy c and b quarks that make up the J/ψ and Υ systems. As would be expected, the model provides more accurate results for the Υ than for the J/ψ. This is understandable in terms of the heavier mass and lower Schroedinger energies of the b quark.

As discussed in Section 2.2, we introduce a convenient scaling of the mass to obtain consistency with the relativistic case. This is achieved by the use of a mass scaling factor β with the property:

$$m = \beta/R.$$

In the model used in this dissertation, β is one of the free parameters available to us, instead of the mass itself.

A further modification made to the bag model is the use of a softened bag. The concept of a non-square wall type of bag has been used before [7], but in this dissertation we confine the gluons to the same soft bag as the quarks, which is a novel approach. We propose a functional form for the soft bag in terms of both a colour dielectric constant and a confining potential. The form is entirely phenomenological, but provides satisfactory results.

We describe the observed J/ψ and T systems within this model. There are three adjustable parameters, namely the bag radius, the coupling constant and the mass scaling factor. We fit each spectrum separately, and thus obtain different values of R, α_s and β for the J/ψ and T. In both cases, the values obtained for these parameters are close to experimental values, as well as those obtained by other models. The α_s values are larger than the MIT value and those obtained in [5] and [6], while the quark masses calculated from the mass scaling factors and the radii lie well within the range of literature values. The bag radii R are physically appealing, although the RMS radii are not as close to experimental values as could be hoped, owing to the form of the potential. We also find that the α_s value for the T is within 20% of the coupling used for the J/ψ. Within the limits of the model, we may conclude that the interaction is reasonably flavour independent, as we would hope.

Once the three adjustable parameters have been determined, we calculate the remainder of the meson spectra. The fit is remarkably good, with no

state more than 5% from the experimental value. The lower states are often within 1%, but the higher states are less precise. Modifications to the potential at higher energies will probably improve the agreement, as discussed in Section 3.10. In addition, we must keep in mind that our model cannot reproduce the widths of the observed states, which imposes a systematic limitation on our theoretical results.

We also determine the wave functions for the calculated states in terms of their components. We find that for both mesons, the ground state is predominantly $|s_{1/2}\ \bar{s}_{1/2}\rangle$, while the upper states are strong mixtures of all the components. The appearance of states that consist only of certain $|q\bar{q}\rangle$ modes is spurious and is probably due to the spin independence of the interaction used in this model.

We find that the soft bag model produces a spectrum that is comparable to the spectra produced by potential models for both mesons. The lower states obtained from the soft bag model are very close to those found using potential models. The higher states of the spectrum calculated with the soft bag model, however, are bunched, which does not occur in the potential models. This is most probably due to the lack of spin-dependent terms in the radial Hamiltonian for the soft bag model.

We do not calculate decay widths for the heavy mesons in this dissertation. Although knowledge of the heavy meson wavefunction alone allows us to calculate the leptonic portion of the decay width, we have not done so as this procedure is not meaningful since the leptonic decay modes are strongly overshadowed by hadronic decay models. (In many cases, upwards of 90% of the total decay width is hadronic in nature [15]). To determine the hadronic portions of the decay widths would require the

calculation of the wavefunctions of all the hadrons produced by these decay modes. For the J/ψ (3100) alone, there are more than fifty hadronic decays. We have thus not attempted to calculate hadronic portions of decay widths for the heavy mesons.

The major source of uncertainty in the soft bag model lies in the choice of potential. There is very little to guide the choice of the potential parameters, and the form given in this dissertation must be regarded as purely ad hoc. In particular, the relationship between the potential and dielectric constant must be viewed as plausible rather than exact.

In conclusion, this dissertation shows that the bag model provides a consistent description of, and acceptable results for, heavy quark systems. We show that a non-relativistic approximation is valid for these systems, although it limits the amount of information available from the calculations. We see that the dynamic interaction is not important for heavy quark systems owing to the low single quark energies in comparison to the gluon modes. Moreover, we show that the physically appealing, although phenomenological, idea of treating the gluons in the same soft bag as the quarks, is acceptable, accurately predicting the spectra of the heavy meson systems studied here.

APPENDIX A

THE MESON WAVEFUNCTIONS

We list the spectra for the mesons and the wavefunctions in the same order as the states appear in the spectrum.

A.1 The J/ψ spectrum and wavefunctions

```
*****************************************
ALPHA =   1.1899999999999995
*****************************************
MESON EIGEN ENERGIES:
  3.5569707816369262 3.1000000000000031
  4.2268877323705638 3.6836771440441350
  4.4303705867196875 3.8611924758376831
  4.5148346618278503 3.9348052910418761
  4.8336472019823291 4.0383537585059655
  4.9300598755689107 4.2966857341545139
  4.9879254848388154 4.3296868767943906
  5.0416889503525086 4.3939736100109742
  5.0949317247022100 4.4403761841721731

MESON EIGEN VECTORS
 0.9603932520375041 83
 0.5581956001854365 95E-01
-0.1882174411253791 51
 0.1882174411253791 51
 0.5349266253960600 04E-02
-0.5798537801429388 79E-01
 0.1193847076854605 89E-01
-0.1193847076854605 98E-01
 0.1181097410995231 21E-02

 0.1716348937687140 61
-0.3055729871990544 44
 0.3851474920994528 98
-0.3851474920994528 62
 0.7343893857996047 49
 0.6114998626375475 63E-01
-0.1347982220970672 52
 0.1347982220970672 56
 0.3288189835395071 22E-01

 0.1049519500935373 05
 0.8309235171120710 75
 0.3680942921929169 50
-0.3680942921929170 05
-0.9145352128411017 58E-01
 0.1203757665263578 97
-0.4710106920443771 13E-01
 0.4710106920443772 17E-01
-0.1653141945465162 96E-01
```

0.5304133086708104655E-14
-0.1886139823749300702E-12
0.6953511269583856649
0.6953511269584444574
-0.1056903721371737716E-12
-0.3304167024995864474E-13
0.1284009744420305651
0.1284009744420303754
-0.6776018292907695986E-14

-0.1863611727668636406
0.4451168766526596651
-0.4175487528453334951
0.4175487528453334034
0.6297363068102533277
0.7239876400907062365E-01
-0.7617045885787360196E-01
0.7617045885787361156E-01
0.6961503980592370936E-01

-0.4707547425047710866E-02
0.5160246494049808816E-01
0.6454426812275478046E-01
-0.6454426812275478046E-01
0.9007147252998003172E-01
-0.2571921494147295585
0.4035580220414238881
-0.4035580220414240889
0.7674661392250300070

0.3835984911268278866E-14
-0.1484456868578294266E-13
-0.1284009744420312712
-0.1284009744420346685
-0.2597415688744500136E-13
0.7404393334836311116E-14
0.6953511269583271341
0.6953511269584585535
0.7162945726091648598E-13

0.3803309639633683966E-01
-0.1067696059794413392
-0.4708840063009987776E-01
0.4708840063009988473E-01
-0.1812371172015218772
0.7238503106400234420
-0.2534092055592481174
0.2534092055592483354
0.5456125210622091771

0.2802815350788173428E-01
-0.3311158553429743668E-01
0.3457631649245802200E-02
-0.3457631649245644668E-02
0.1214590049765973382
0.6188179226575879110
0.4965794600023186687
-0.4965794600023190076
-0.3272615620753858898

A.2 The Υ spectrum and wave functions

```
*****************************************
ALPHA = 0.9799999999999999996
*****************************************
MESON EIGEN ENERGIES
  8.6146194483335853          9.4599999999999996
  9.1277189512812408 9          10.0234516216075955
  9.2658867306044810 1          10.1748488133708772
  9.3225984896367201 6          10.2374531248924787
  9.4098395530434006          10.3334162061448706
  9.6147887358398730 1          10.5583189478986499
  9.6399945236985916 1          10.5858886444264901
  9.6903284020744613 3          10.6412717628934219
  9.7281748432482352 2          10.6795377963789090

MESON EIGEN VECTORS
 0.9570685978903878186
 0.5898568062634918415 -01
-0.1965457918995536 51
 0.1965457918995536 51
 0.1182643340435830 56E-01
-0.5371091919072254 98E-01
 0.1133832225798956 51E-01
-0.1133832225798956 71E-01
 0.1259982287884241 17E-02

 0.1699917919980809 96
-0.3042056022853678 88
 0.3742474338234542 95
-0.3742474338234542 34
 0.7448626793193418 34
 0.6243041504762212 89E-01
-0.1367273134006574 91
 0.1367273134006571 16
 0.3529664524478905 08E-01

 0.1059180197228246 99
 0.8374520003426325 74
 0.3606118682804614 20
-0.3606118682804607 54
-0.7310680879724536 23E-01
 0.1300635231742847 95
-0.4940260470362958 80E-01
 0.4940260470362958 76E-01
-0.1520923649650339 23E-01

 0.6044549767512540 34E-15
-0.5870507706084723 08E-12
 0.6953904760745465 43
 0.6953904760748136 77
-0.3007613378425080 09E-12
-0.1122221085907692 73E-12
 0.1281876974777694 94
 0.1281876974777694 14
-0.3228912730945360 32E-13
```

-0.205308296978176472
0.432230642785473778
-0.429194101457299609
0.429194101457299582
0.618254257922199786
0.637301138120449084E-01
-0.741679601468114060E-01
0.741679601466110313E-01
0.727262868343296316E-01

-0.13346 305508575444E-02
0.503286594191573652E-01
0.664309533813207814E-01
-0.664309533813205288E-01
0.866696436189551186E-01
-0.249214487211533053
0.398472835168291309
-0.398472835168290337
0.775537629322701106

-0.980728974995328612E-15
0.396184755027967376E-13
-0.128187697477655183
-0.128187697477700521
0.887964655506550873E-13
-0.230273044879934645E-13
0.695390476074809596
0.695390476074852925
-0.387709604125035795E-12

0.346310673217403893E-01
-0.110401728756755149
-0.514128253723694668E-01
0.514128253723592724E-01
-0.180306486977018593
0.740705657310064186
-0.248684288678897589
0.246684288678897242
0.527698915090420382

0.234792218471144773E-01
-0.332530922762805953E-01
0.193997751949152273E-02
-0.193997751949124522E-02
0.132050245823358975
0.601237724656724477
0.503041890638250605
-0.503041890638251132
-0.336614730731080863

REFERENCES

1. T.D. Lee, Particle Physics and introduction to Field Theory. (Harwood, Chur. 1981).

2. A. Chodos, R.L. Jaffe, K. Johnson, C.B. Thorn and V.F. Weisskopf, Phys. Rev. D, 9, 3471 (1974).

3. W.A. Bardeen, M.S. Chanowitz, S.D. Drell, M. Weinstein and T.M. Yan, Phys. Rev. D, 11, 1094 (1975).

4. H. Eggers, M.Sc. Dissertation, Pretoria (1985).

5. J.F.H. Quick and W.D. Heiss, J. Phys. G: Nucl. Phys, 13, 1201 (1987).

6. M.Z.I. Gering, Ph.D. Thesis, Johannesburg (1985).
M.Z.I. Gering and W.D. Heiss, Phys. Rev. D, 33, 1980 (1986).

7. V. Bernard, R. Brockmann, M. Schaden, W. Weise and E. Werner, Nucl. Phys. A. 412, 349 (1984).

8. T. DeGrand, R.L. Jaffe, K. Johnson and J. Kiskis, Phys. Rev. D, 12, 2060 (1975)

9. J.D. Jackson, Classical Electrodynamics, John Wiley and Sons, Inc. (1975).

10. M.L. Boas, Mathematical Methods in the Physical Sciences, John Wiley and Sons, Inc. (1983).

11. M. Abramowitz and I.A. Stegun (Editors), Handbook of Mathematical Functions with Formulas, Graphs and Mathematical Tables, NBS, AMS55 (U.S. Government Printing Office, Washington D.C., 1964).

12. R.D. Viollier, S.A. Chin and A.K. Kerman, Nucl. Phys. A 407, 269 (1983).

13. W.D. Heiss, C.A. Engelbrecht and F.J.W. Hahne, Ann. Phys. (NY) 104, 274 (1977).

14. C.F. Vermaak, D. Vermaak and H.G. Miller, Comput. Phys. Commun. 31, 41 (1984).

15. Particle Data Group: Review of Particle Properties, Rev. Mod. Phys., 56 2 Part II.

16. W. Kwong, J.L. Rosner and C. Quigg, Ann. Rev. Nucl. Part. Sci. 37. 325 (1987).

17. K. Königsman, Phys. Rep. 139 5, 244 (1986).

18. C. Quigg and J.L. Rosner, Phys. Rep. 56 4, 167 (1979).

19. O. Portilho and Z.M.O. Shokranian, Revista Brasileira de Fisica 14 1, 15 (1984).

20. D.S. Kulshreshtha and R.S. Kaushal, Phys. Rev. D 26, 2331 (1982).

21. D.P. Stanley and D. Robson, Phys. Rev. D 21, 3180 (1980).

22. J.L. Richardson, Phys. Lett. 82B, 272 (1979).

23. E. Eichten et. al., *Phys. Rev. D 21, 203 (1980).*

24. C.S. Kalman and N. Mukerji, Phys. Rev. D 27, 2114 (1983).

25. J. Dias de Deus, Phys. Lett. 98B, 301 (1981).

26. A. Martin, Phys. Lett. 93B, 338 (1980).

27. N. Barik and S.N. Jena, Phys. Lett. 97B, 261 (1980).

28. S.P. Khare, Phys. Lett. 137B, 422 (1984).

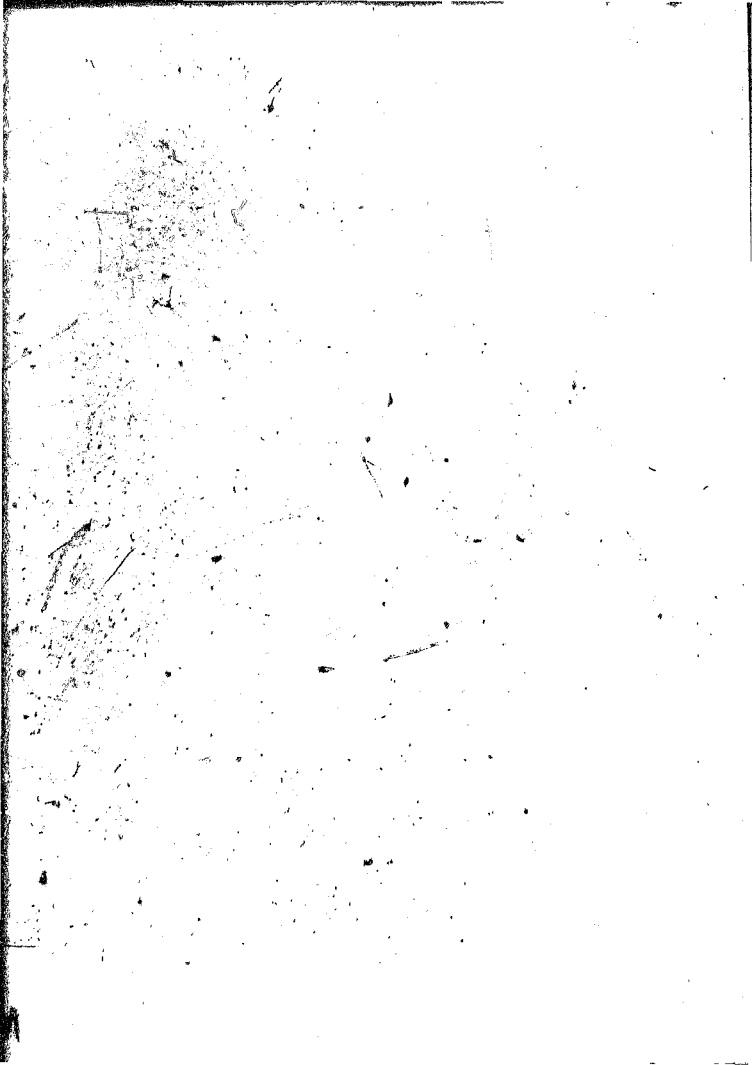

Author Davidson Neil John
Name of thesis Heavy Mesons In The Bag Model. 1988

PUBLISHER:
University of the Witwatersrand, Johannesburg
©2013

LEGAL NOTICES:

Copyright Notice: All materials on the University of the Witwatersrand, Johannesburg Library website are protected by South African copyright law and may not be distributed, transmitted, displayed, or otherwise published in any format, without the prior written permission of the copyright owner.

Disclaimer and Terms of Use: Provided that you maintain all copyright and other notices contained therein, you may download material (one machine readable copy and one print copy per page) for your personal and/or educational non-commercial use only.

The University of the Witwatersrand, Johannesburg, is not responsible for any errors or omissions and excludes any and all liability for any errors in or omissions from the information on the Library website.